



Universiteit
Leiden
The Netherlands

Glucocorticoid modulation of the immune response: Studies in zebrafish

Xie, Y

Citation

Xie, Y. (2020, November 26). *Glucocorticoid modulation of the immune response: Studies in zebrafish*. Retrieved from <https://hdl.handle.net/1887/138400>

Version: Publisher's Version

License: [Licence agreement concerning inclusion of doctoral thesis in the Institutional Repository of the University of Leiden](#)

Downloaded from: <https://hdl.handle.net/1887/138400>

Note: To cite this publication please use the final published version (if applicable).

Cover Page



Universiteit Leiden



The handle <http://hdl.handle.net/1887/138400> holds various files of this Leiden University dissertation.

Author: Xie, Y.

Title: Glucocorticoid modulation of the immune response: Studies in zebrafish

Issue Date: 2020-11-26

Chapter 5

Liposome encapsulation of prednisolone phosphate improves its therapeutic ratio in a zebrafish model for inflammation

Yufei Xie, Panagiota Papadopoulou, Björn de Wit, Jan C. d'Engelbronner, Patrick van Hage, Fred Campbell, Alexander Kros, Marcel J.M. Schaaf

Abstract

Glucocorticoids (GCs) are effective anti-inflammatory drugs, but their clinical use is limited by the severity of their side effects. Using liposomes to deliver GCs at inflammatory sites in the body is a promising approach to improve the therapeutic ratio of these drugs. In this study, we demonstrate that zebrafish embryos provide a useful tool to determine the therapeutic effects and possible side effects of liposomal formulations of GCs. We used a wound-induced inflammation model to investigate liposome encapsulation of the GC prednisolone phosphate (PLP). First, we studied the biodistribution of liposomes with different formulations. Our results showed that macrophage-targeting liposomes composed of 20% 1,2-distearoyl-*sn*-glycero-3-phospho-*rac*-(1-glycerol) (DSPG), 50% 1,2-dioleoyl-*sn*-glycero-3-phosphocholine (DOPC) and 30% cholesterol accumulated in macrophages, whereas PEGylated liposomes (with polyethylene glycol (PEG) polymers on their surface) remained in circulation for longer periods of time without being scavenged. Upon laser wounding of the tail, accumulation near the wounding site was observed for both liposomes. Furthermore, encapsulation of PLP in the macrophage-targeting and the PEGylated liposomes increased the potency of its inhibition of the migration of neutrophils towards the wound. In contrast, encapsulation of PLP in either type of liposome reduced its inhibitory effects on tail fin regeneration, and encapsulation in the PEGylated liposome attenuated the activation of glucocorticoid responsive reporter genes throughout the body. In conclusion, using a zebrafish model for inflammation we have shown that encapsulation of PLP in liposomes enhances its anti-inflammatory effects and decreases undesired effects in the rest of the body and the regeneration of the affected tissue.

Introduction

Glucocorticoids (GCs) are a class of steroid hormones secreted by the adrenal gland. Due to their potent anti-inflammatory effects, synthetic GCs are widely prescribed for treating immune-related diseases, such as asthma, rheumatoid arthritis (RA), dermatitis and several autoimmune diseases [1, 2]. Through activation of an intracellular receptor, the glucocorticoid receptor (GR), GCs regulate a wide variety of systems in our body, including the immune system, metabolism, bone formation and central nervous system, leading to side effects such as infectious diseases, diabetes, osteoporosis and depression, which severely limits the clinical use of these widely prescribed anti-inflammatory drugs [3]. Using local administration approaches, such as intra-articular injection, inhalation and topical treatment, these side effects could be alleviated to some extent, but these methods are applicable for only a limited number of diseases [4].

Using nanoparticles to achieve targeted delivery of drugs is a promising approach to increase the specificity of a drug and reduce its side effects since it may enable the use of lower therapeutic doses [5, 6]. There are two major types of targeted delivery approaches: active targeting and passive targeting. Active targeting is generally achieved by modifying the surface of the particles with specific targeting molecules, such as antibodies, peptides, or carbohydrates, which may be recognized by antigens or other molecules on the membranes of specific cells so the drugs can be released at a desired location [6]. The surface of passive targeting nanoparticles is generally not altered with targeting molecules. The targeting could be dependent on the enhanced permeation and retention (EPR) effect which is observed in tumors and inflammatory sites due to the locally increased permeability of the vasculature [7]. The uptake by migratory phagocytes like macrophages which are recruited by an inflamed tissues may also contribute to the targeting. The efficacy and specificity of targeting may be influenced by several physicochemical properties of the nanoparticles, including the size, shape, surface charge, composition and surface modification [8-10].

Liposomes are spherical vesicles composed of lipids and widely used to deliver therapeutic molecules, of which the composition can be manipulated easily [11, 12]. One frequently studied formulation of passive targeting liposomes uses phospholipids linked to a polymer polyethylene glycol (PEG) chain [13, 14]. The PEGylation prevents the liposome from being recognized by serum proteins such as complement proteins, immunoglobulins and non-immune opsonins, thereby avoiding opsonization and clearance, thus, increasing the half-life in the circulation [15]. A lot of efforts have been made to explore PEGylated liposome-encapsulated GCs. One widely investigated formulation is using PEG2000-DSPE, DPPC and cholesterol for liposome assembly, and the water-soluble GC prednisolone phosphate (PLP) as the loaded drug [16, 17]. In a rodent model of RA, the PEGylated liposome-encapsulated PLP remained in the circulation longer than free PLP and accumulated in the inflamed joints, resulting in enhanced therapeutic effects compared to free PLP [16, 18].

Similar results were obtained using other rodent models for inflammation-related diseases such as atherosclerosis [19], multiple sclerosis [13] and cancer [20]. Attempts to improve the therapeutic effects include using different synthetic GCs [21-23], conjugation with targeting molecules [24-27], optimization of formulation [28, 29] and co-treatment with anti-tumor drugs [30]. However, obstacles still exist, such as unwanted off-target accumulation in spleen, liver and kidney [18, 31], a certain level of GCs-induced side effects [22, 23], and an unexpected lack of anti-inflammatory effect when applied clinically [32]. Therefore, novel tools are needed, which can be used for rapid screening of the biodistribution, therapeutic effects and side effects of different liposomal formulations of GC drugs.

Macrophages are critical components of the inflammatory response and represent one of the target cells for the treatment of inflammatory diseases. Macrophage targeting can be achieved by modifying the surface of nanoparticles with targeting molecules such as folate, which can be recognized by overexpressed folic acid receptor (FR) in tumor-associated macrophages [33, 34], or mannose residues, which interact with the mannose receptor mainly present on the surface of macrophages [35, 36], or anti-CD163 antibodies, which target CD163 positive macrophages [37, 38]. Moreover, targeted delivery of GCs to macrophages has also been reported by using inorganic-organic hybrid nanoparticles, which were preferentially taken up by macrophages and showed full therapeutic efficacy in a mouse multiple sclerosis model [39].

Over the last decades, the zebrafish has emerged as a useful *in vivo* model for biomedical research, complementary to rodent models due to several characteristics, such as their short generation time, small size, and optical transparency. In addition, the sequencing of the zebrafish genome [40], the availability of various genetic tools [41] and their well-conserved immune system [42] have contributed to the popularity of this animal model. Due to the similarity of the GC signaling pathway between humans and zebrafish, the zebrafish model is highly suitable for studying the effects and mechanisms of GC action *in vivo*, particularly their anti-inflammatory effects [43-45]. Recently, the zebrafish has been used for studies on liposomal drug delivery. In these studies, zebrafish embryos were utilized to determine the biodistribution of fluorescently labeled liposomes with different formulations and to unravel the mechanisms underlying their uptake in specific cell types [46, 47].

In the present study, we have used the zebrafish embryo as a model system to study the biodistribution of liposomes, and their possible use for improving the therapeutic ratio of GC drugs. A new macrophage-targeting liposome formulation was generated and this liposome was shown to behave differently from a PEGylated liposome, although both of them were shown to accumulate at sites of inflammation. In addition, we demonstrate that the encapsulation of PLP in both the macrophage-targeting and the PEGylated liposomes enhances the anti-inflammatory effects of the GC, whereas it decreases possible adverse effects.

Results

Optimization and characterization of macrophage-targeting liposomes

In order to optimize the formulation of macrophage-targeting liposomes, fluorescently labeled liposome formulations were prepared with different ratios of the anionic phospholipid 1,2-distearoyl-*sn*-glycero-3-phospho-*rac*-(1-glycerol) (DSPG) and cholesterol (10:40%, 15:35%, 20:30%, 25:25%, 30:20%), combined with 50% of the neutrally charged, non-saturated 1,2-dioleoyl-*sn*-glycero-3-

phosphocholine (DOPC). This formulation originates from a marketed liposomal product (AmBisome), which is composed of DSPG, cholesterol and 1,2-distearoyl-*sn*-glycero-3-phosphocholine (DSPC) (ratio 21:26:53), and used for treating fungal infections [48, 49]. In preliminary studies, it was found that replacing the saturated phospholipid DSPC with the unsaturated DOPC, macrophage targeting of the liposome was observed in zebrafish embryos (unpublished data).

The liposomes with different DSPG:cholesterol:DOPC ratios were injected intravenously in 2 days post fertilization (dpf) zebrafish embryos from the *Tg(mpeg1:GFP)* line, in which the macrophages are fluorescently labeled. At 2 hours post injection (hpi), confocal microscopy images were taken to study the biodistribution of the liposomes, and representative images are shown in Figure 1A-F. Using the images, we quantitated the number and percentage of macrophages that contained liposomes. The results show that a higher percentage of DSPG in the liposome formulation increases the macrophage targeting efficiency of the liposomes (Figure 1G,H). Simultaneously, we observed association of liposomes with endothelial cells (ECs) of the posterior cardinal vein (PCV), the caudal vein (CV) and the caudal hematopoietic tissue area (CHT). To quantitate this effect, we determined the ratio between the signal in the region encompassing the CHT and CV and the region dorsally from this area, which showed that increasing the DSPG percentage to 25% enhanced targeting of the liposomes to the region encompassing the CHT and CV (Figure 1I). The uptake of liposomes by cells in this region is considered an off-target accumulation, since the endothelial cells (ECs) in this area have been shown to be a functional equivalent of the liver sinusoidal/scavenger endothelial cells (LSECs) in mammals [47]. The total number of macrophages in the embryonic body is not significantly influenced by the variation in DSPG percentages (Supplementary Figure 1A). After comparing the biodistribution of the different liposomes, the 20% DSPG liposome was considered as the optimal formulation since it displays the highest ratio between macrophage targeting and CHT localization.

To characterize the behavior of the 20% DSPG liposomes in further detail, we injected these liposomes in embryos at different ages (1, 2 and 3 dpf), and imaged their biodistribution two hours after the injection (Figure 2A-F). From the images, we quantified the number and percentage of macrophages that contained liposomes. The macrophage targeting property of the 20% DSPG liposome was observed at all ages. After injection at 1 and 2 dpf, around 64% of the macrophages had taken up liposomes (with a lower absolute number of macrophages at 1 dpf), and at 3 dpf approximately 35% of all macrophages contained liposomes. (Figure 2I-J, Supplementary Figure 1B). For comparison, PEGylated liposomes (formulation: DPPC(62%)/PEG-DSPE(5%)/cholesterol(33%)) were injected in 3 dpf embryos. In contrast to the 20% DSPG liposomes, we observed that PEGylated liposomes remained freely circulating in the vasculature, and were not taken up by macrophages (Figure 2G-H), which was reflected in a significantly lower percentage of the macrophages containing PEGylated liposomes

(approximately 6%, Figure 2I-J). No difference in the total macrophage number was observed between larvae injected with 20% DSPG and PEGylated liposomes at 3 dpf (Supplementary Figure 1B). In addition, liposomes containing PLP behaved similarly to empty liposomes (Supplementary Figure 2).

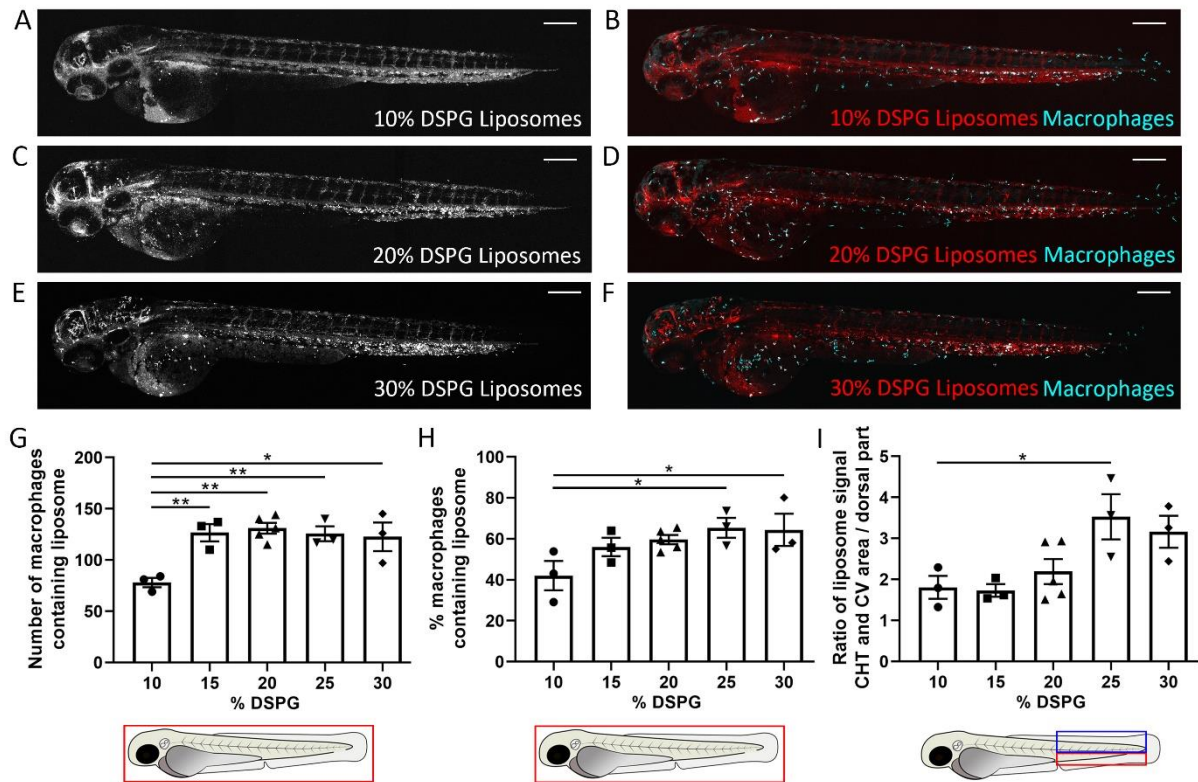


Figure 1. Biodistribution of macrophage-targeting liposomes with different formulations in zebrafish embryos.

A-F. Representative images of *Tg(mpeg1:GFP)* embryos injected with liposomes containing different percentages of DSPG at 2 days post fertilization (dpf). Confocal microscopy images were taken at 2 hours post injection (hpi). Liposomes are shown in red and macrophages in cyan (B,D,F). Scale bar = 200 μ m. G-H. The number (G) and percentage (H) of macrophages containing liposomes quantified in the whole body. A significant difference was observed for the number of macrophages containing liposomes with DSPG percentages of 15% to 30% compared to 10%. For the percentage of macrophages containing liposomes, a significant difference was observed for the 25% and 30% DSPG liposomes compared to the 10% DSPG liposome. I. The ratio between the (fluorescent) signal of liposomes in the area, indicated by the red box, encompassing the caudal vein (CV) and the caudal hematopoietic tissue (CHT) and the signal in the dorsal part of the tail (indicated by the blue box). A significant difference was observed between injection with 25% DSPG liposomes compared to 10% DSPG liposomes. Statistical analysis was performed by one-way ANOVA with Bonferroni's post hoc test. Data shown are the means \pm s.e.m. of 3-5 individual embryos, of which the individual data are indicated. Statistically significant differences between groups are indicated by: * $p < 0.05$; ** $p < 0.01$.

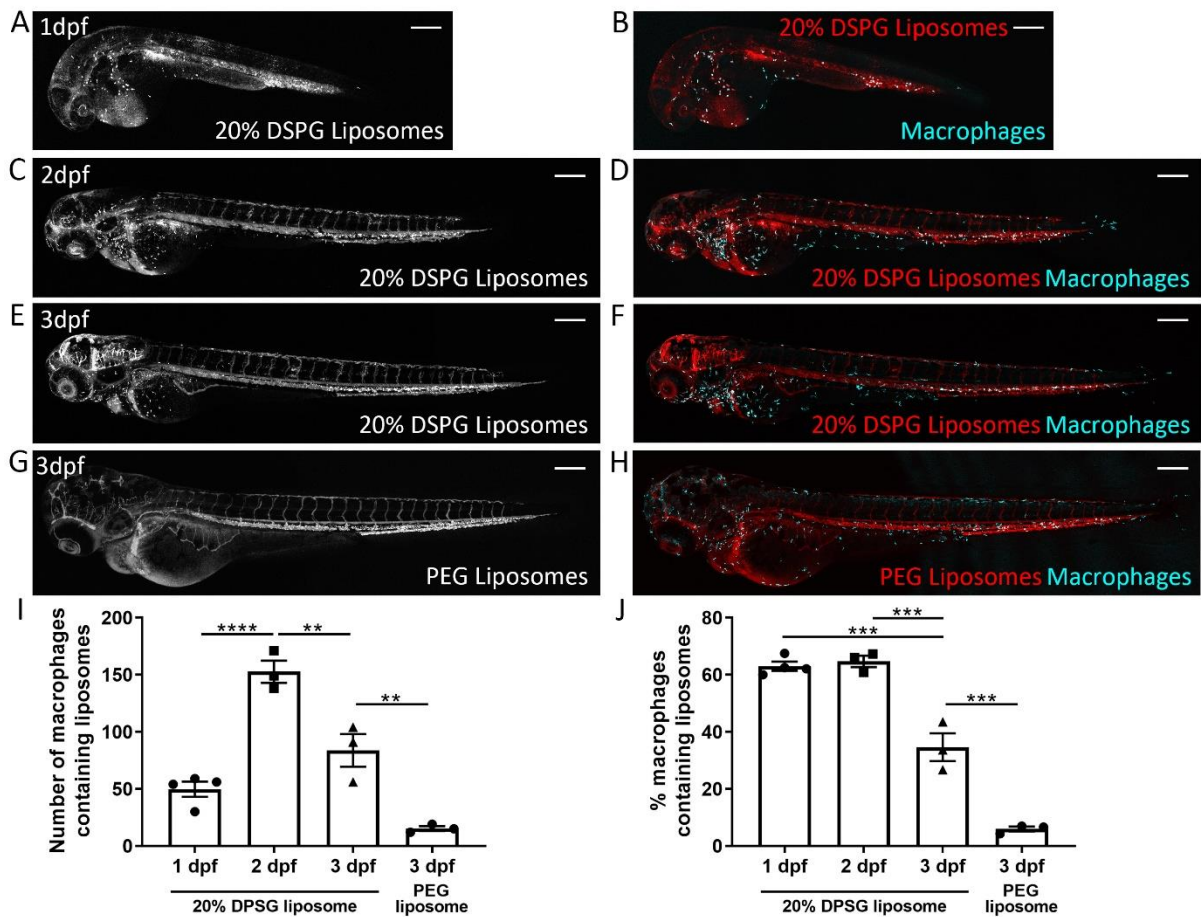


Figure 2. Biodistribution of liposomes in zebrafish embryos at different stages of development. A-H. Representative images of embryos of the *Tg(mpeg1:GFP)* line injected with 20% DSPG liposomes at 1 (A), 2 (B) or 3 dpf (C) or with PEGylated liposomes at 3 dpf (D). Confocal microscopy images were taken at 2 hpi. Liposomes are shown in red and macrophages in cyan (B,D,F,H). Scale bar = 200 μ m. I-J. The number (I) and percentage (J) of macrophages containing liposomes quantified in the whole body of embryos injected with 20% DSPG liposomes at 1, 2 or 3 dpf or with PEGylated liposomes at 3 dpf. Statistical analysis by one-way ANOVA showed a significantly lower number and percentage of macrophages containing liposomes when injected with PEGylated liposomes at 3 dpf, compared to injection with 20% DSPG liposomes. Upon injection with 20% DSPG liposomes, at 1 and 3 dpf significantly lower numbers of macrophages containing liposomes were observed than at 2 dpf. Embryos at 3 dpf showed significantly lower percentages of macrophages containing liposomes compared to embryos at 1 and 2 dpf. Data shown are the means \pm s.e.m. of 3-4 individual embryos, of which the individual data are indicated. Statistically significant differences between groups are indicated by: ** $p < 0.01$; *** $p < 0.001$; **** $p < 0.0001$.

Biodistribution of liposomes upon laser wounding

To study targeting of liposomes towards an inflammatory site, we damaged the tail of 3 dpf embryos from the *Tg(mpeg1:GFP)* line by laser irradiation (Figure 3A), and injected different fluorescently labeled liposomes (20% DSPG or PEGylated) immediately after the laser wounding. Confocal microscopy images were taken at 4 hours post wounding (hpw). In all images, accumulation of macrophages was observed near the wounded area (Figure 3B-E). In the embryos injected with the 20% DSPG liposomes, most of these macrophages that had accumulated near the wounded area contained liposomes (Figure 3B,C). In the embryos injected with PEGylated liposomes, most of the macrophages near the wound site did not contain any liposomes, but accumulation of liposomes was observed in the wounded area with a diffuse pattern (Figure 3D). As a control for the integrity of the vascular system, the polysaccharide dextran (2,000,000 MW) was injected. No accumulation of dextran was observed near the wounded site (Figure 3E), suggesting that the accumulation of the PEGylated liposomes is not caused by local damage to the vascular system but is due to the inflammation-induced change in vesicle permeability. When we quantitated the percentages of macrophages containing liposomes in the area near the laser wound, we again found a very low percentage ($3.2 \pm 2.0\%$) in embryos injected with PEGylated liposomes, and a higher percentage ($39.0 \pm 5.2\%$) in the 20% DSPG liposome injected embryos (Figure 3F).

Effect of PLP and encapsulated PLP on wounding-induced neutrophil migration

Since it has been shown that macrophage migration towards a wounded site is not affected by GC treatment in zebrafish, but that the neutrophil migration is inhibited [50, 51], we used the accumulation of neutrophils at the wounded area as a readout for the anti-inflammatory effect of PLP. For this purpose, we applied laser wounding in 3 dpf embryos from the *Tg(mpx:GFP)* line, in which neutrophils are fluorescently labeled. At different time points after the wounding, fluorescence microscopy images were taken and the neutrophil accumulation in a defined area of the tail was quantitated (Figure 4A-B). The results showed that laser wounding induced a rapid increase in the number of accumulated neutrophils at early time points (from 0 to 4 hpw) and then the number decreased gradually between 4 and 24 after wounding (Supplementary Figure 3). Subsequently, using the number of neutrophils at the site of laser injury at 4 hpw as a readout, we studied the anti-inflammatory effect of free PLP and liposome-encapsulated PLP. Injection of free PLP (0.04, 0.2, 1, 5 and 25 pmol per embryo) resulted in a dose-dependent inhibition of the neutrophil migration, with a significant inhibitory effect observed for the 5 and 25 pmol doses ($23.4 \pm 3.6\%$ and $30.9 \pm 4.2\%$ inhibition respectively) (Figure 4C). Injection of PLP encapsulated in 20% DSPG liposomes (at doses of 0.04, 0.2 and 1 pmol) also inhibited neutrophil migration dose-dependently, and showed a significant inhibition

already at a dose of 0.2 pmol ($21.0 \pm 4.7\%$) (Figure 4D). Injection of PLP encapsulated in PEGylated liposomes resulted in a significant inhibition only at the 1 pmol dose ($21.4 \pm 6.0\%$) (Figure 4E). These results indicate that PLP shows a more potent anti-inflammatory effect when encapsulated in a liposome, with the 20% DSPG liposome showing a slightly higher potency than the PEGylated liposome.

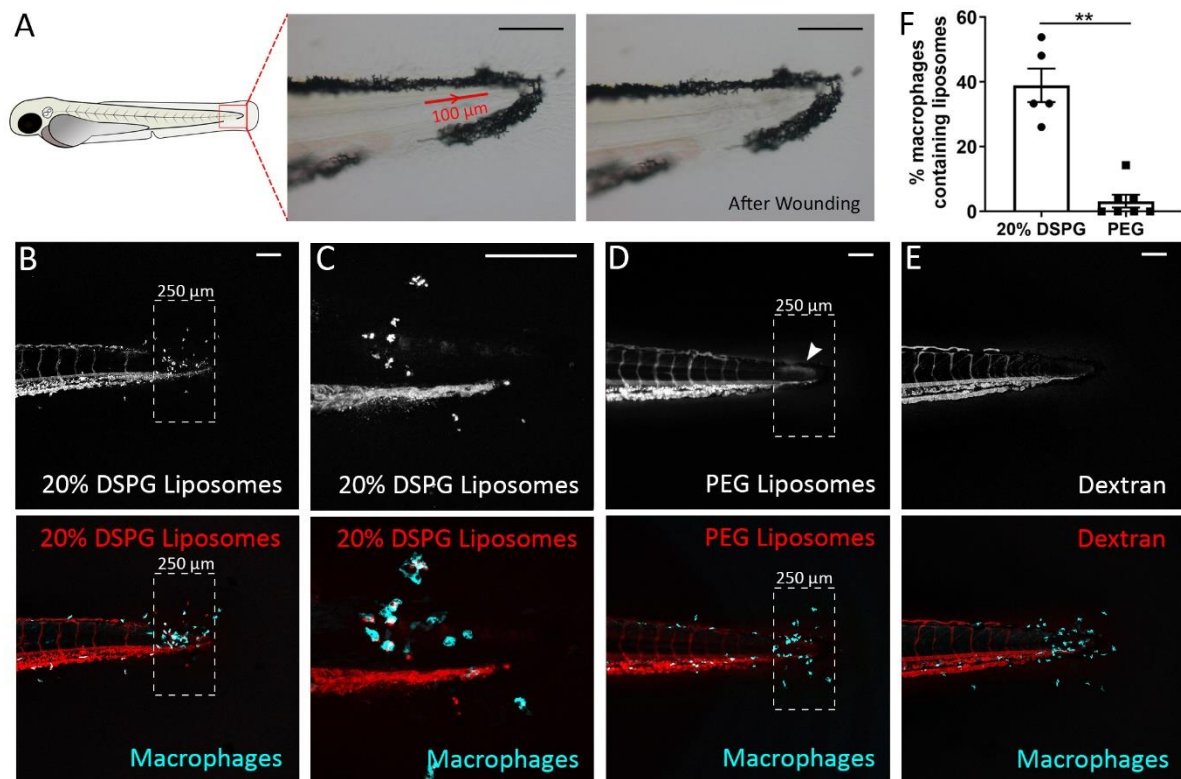


Figure 3. Laser wounding in zebrafish embryos and the subsequent accumulation of liposomes at the wounded site. A. Schematic drawing of a zebrafish embryo at 3 dpf, and brightfield microscopy images showing the position and size of the area exposed to laser irradiation (red line with arrow indicating the direction of laser) and the damaged tissue after the laser wounding procedure. B-E. Representative confocal microscopy images of tail regions from 3 dpf embryos of the *Tg(mpeg1:GFP)* line, subjected to laser wounding and injected with 20% DSPG liposomes (B and C, with C at a higher magnification), PEGylated liposomes (D), or dextran (2,000,000 MW, E). The dashed box indicates the area where damage and accumulation of neutrophils were seen. The white arrowhead indicates the accumulation of PEG liposomes (D). Images were taken at 4 hours post wounding (hpw). The dashed box shows the area of quantification. Liposomes are shown in red and macrophages in cyan. Scale bar = 100 μm. F. The percentage of macrophages containing liposomes in the area near the laser wound (dashed box), in embryos injected with 20% DSPG or PEGylated liposomes. Statistical analysis by two-tailed t-test showed a significantly higher percentage of macrophages containing liposomes upon injection with 20% DSPG liposomes. Data shown are the means \pm s.e.m. of 5-7 individual embryos, of which the individual data are indicated. Statistically significant differences between groups are indicated by: ** $p < 0.01$.

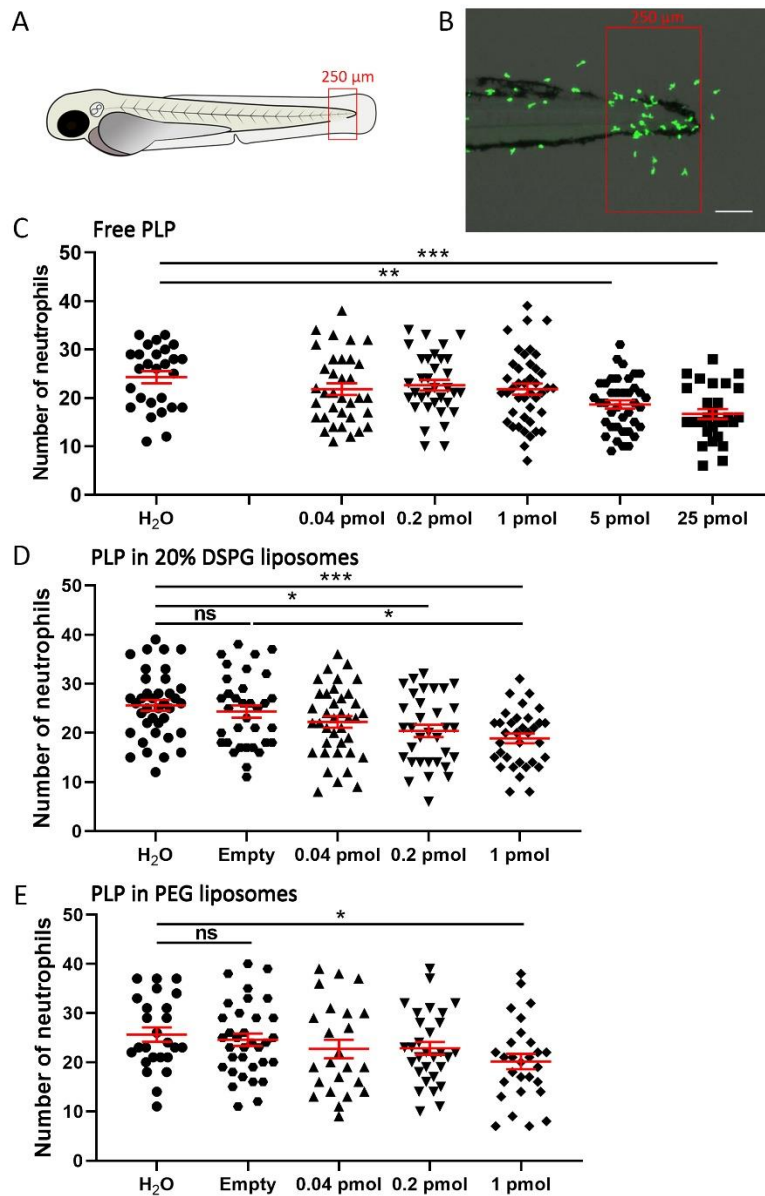


Figure 4. Effect of free and liposome-encapsulated PLP on neutrophil recruitment upon laser wounding.

Tg(mpx:GFP) embryos (at 3 dpf) were subjected to the laser wounding procedure and injected with different doses of free or liposome-encapsulated PLP, and fluorescence microscopy images were taken at 4 hpw. A. Schematic drawing of a zebrafish embryo at 3 dpf indicating the area in which the recruited neutrophils were counted (red box). B. Representative image showing the accumulation of neutrophils (green) near the wound. Scale bar = 100 μ m. C-E. The number of neutrophils recruited to the wounded area at 4 hpw are shown after injection of different doses of free PLP (C), PLP encapsulated in 20% DSPG liposomes (D) and PLP encapsulated in PEGylated liposomes (E). H₂O and empty liposomes were injected as control. Statistical analysis was performed by one-way ANOVA with Bonferroni's post hoc test. A significant inhibition of the neutrophil migration was observed when embryos had been injected with 5 or 25 pmol of free PLP, 0.2 or 1 pmol of PLP encapsulated in 20% DSPG liposomes and 1 pmol of PLP encapsulated in PEGylated liposomes. Each data point represents a single embryo and the means \pm s.e.m. of data accumulated from three independent experiments are shown in red. Statistically significant differences between groups are indicated by: ns, non-significant; * $p < 0.05$; ** $p < 0.01$; *** $p < 0.001$.

Effects of PLP and encapsulated PLP on tissue regeneration and transactivation

To develop novel anti-inflammatory GC therapies, it is important to study possible side effects of the treatment as well. In this study, we first investigated the effect of free PLP and encapsulated PLP on tissue regeneration. We performed tail fin amputation on 2 dpf embryos (Figure 5A) and injected the amputated embryos with different doses of free PLP or liposome-encapsulated PLP immediately after the amputation. The length of the regenerated tail fin was measured at 36 hour post amputation (hpa). Free PLP showed a significant inhibitory effect on regeneration at all doses tested (from 0.04 pmol ($3.4\pm 1.0\%$) to 25 pmol ($30.5\pm 3.1\%$)) and this effect was dose-dependent (Figure 5B,E). For PLP encapsulated in 20% DSPG liposomes, a significant inhibition was observed when the injected dose was 1 pmol ($5.7\pm 1.4\%$), but not at lower doses (0.04 pmol and 0.2 pmol) (Figure 5C). When the embryos were injected with PLP encapsulated in PEGylated liposomes, no significant effect of the treatment was observed (Figure 5D). These results indicate that encapsulation of PLP in liposomes decreases the inhibitory effect of PLP on regeneration, showing even an absence of inhibition for the PEGylated liposomes at the doses tested.

Subsequently, we studied the effect of free and liposome-encapsulated PLP on the transactivation of a glucocorticoid response element (GRE)-containing promoter. For this purpose, we used the *Tg(9xGRE-HSV.U123:EGFP)* reporter line, in which the EGFP gene is driven by a GRE-containing promoter. This way, we were able to quantify the systemic induction of the transactivation properties of the Gr by the GC treatment, by quantitating the EGFP signal throughout the embryonic body. Embryos were injected with free PLP and liposome-encapsulated PLP at 3 dpf, and fluorescence microscopy images were taken at 24 hpi. The quantitated EGFP signals showed that both free and liposome-encapsulated PLP induced significant dose-dependent increases in the level of GFP expression (Figure 6). However, for free PLP a significant increase was already observed at a dose of 0.2 pmol ($26.1\pm 2.6\%$), whereas for both the 20% DSPG and the PEGylated liposome-encapsulated treatments a significant increase was only observed for the 1 pmol dose ($44.5\pm 3.4\%$ and $6.2\pm 3.1\%$ respectively). These data demonstrate that liposome encapsulation decreases the potency of PLP to induce the transactivation activity of the Gr throughout the body of zebrafish embryos.

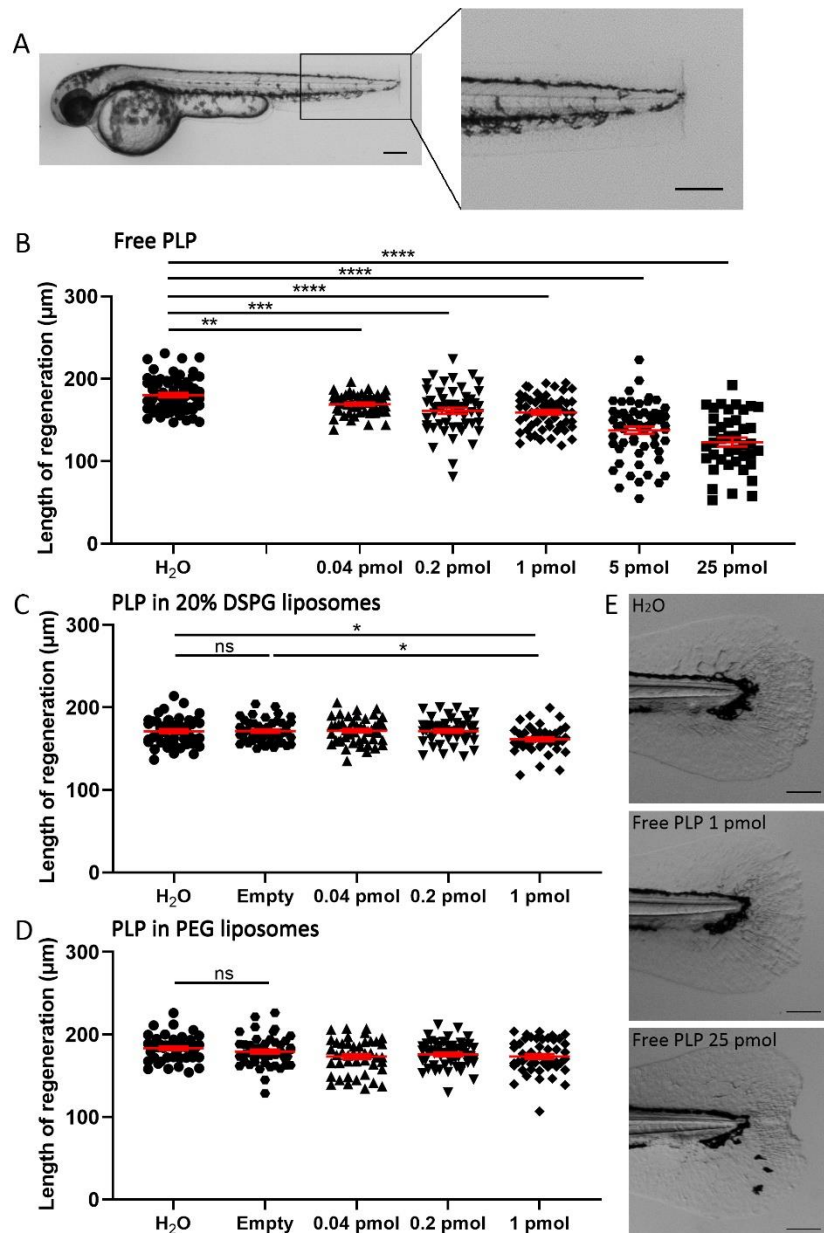


Figure 5. Effect of free and liposome-encapsulated PLP on regeneration of the tail fin after amputation. Embryos (at 2 dpf) were subjected to the tail fin amputation procedure and injected with different doses of free or liposome-encapsulated PLP. **A.** Representative image of a 2dpf zebrafish embryo immediately after amputation, showing the position of the amputated part of the tail fin. Scale bar = 200 µm. **B-D.** The length of the regenerated tail fin, measured at 36 hour post amputation (hpa), are shown after injection of different doses of free PLP (**B**), PLP encapsulated in 20% DSPG liposomes (**C**) and PLP encapsulated in PEGylated liposomes (**D**). H₂O and empty liposomes were injected as control. Statistical analysis was performed by one-way ANOVA with Bonferroni's post hoc test. Significant inhibition of the tail fin regeneration was observed when embryos had been injected with 0.04-25 pmol of free PLP or 1 pmol of PLP encapsulated in 20% DSPG liposomes. No significant inhibition was observed after injection with PLP encapsulated in PEGylated liposomes. Each data point represents a single embryo and the means ± s.e.m. of data accumulated from three independent experiments are shown in red. Statistically significant differences between groups are indicated by: ns, non-significant; * p<0.05; ** p<0.01; *** p<0.001; **** p<0.0001. **E.** Representative images of regenerated tail fins at 36 hpa for embryos injected with H₂O, 1 pmol PLP or 25 pmol PLP. Scale bar = 100 µm.

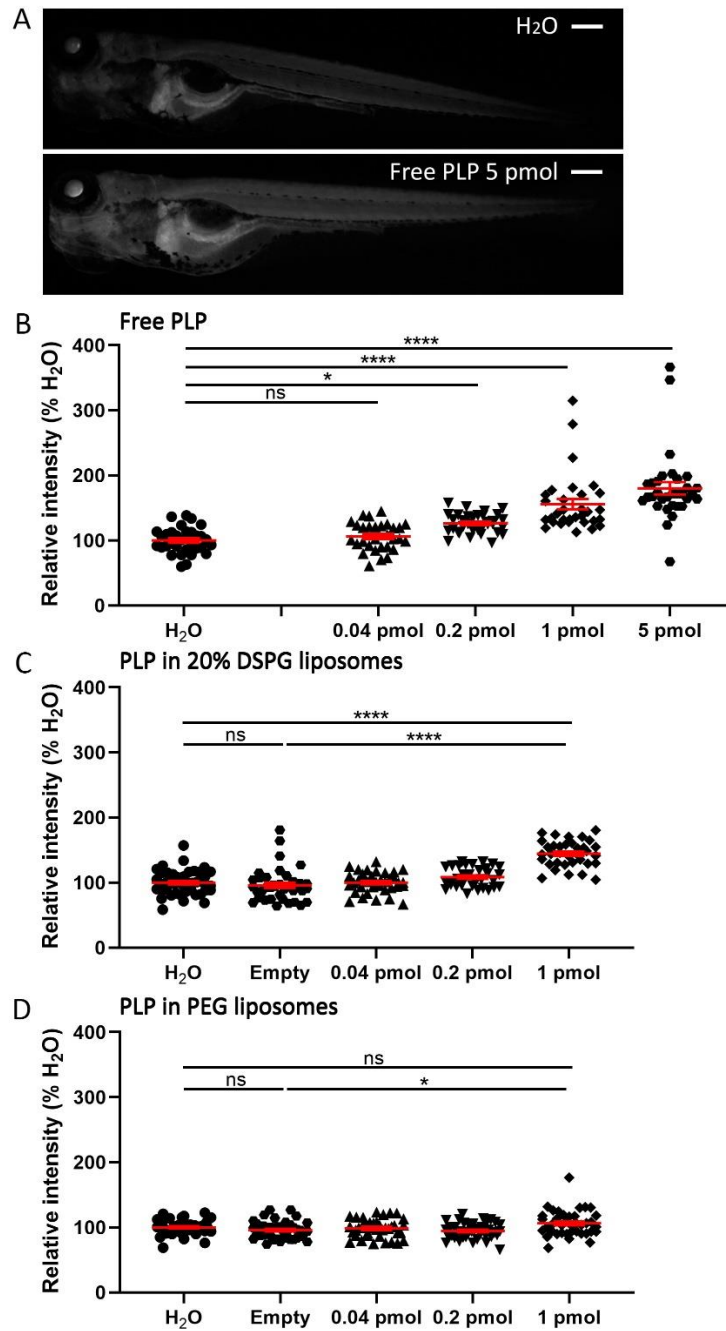


Figure 6. Effect of free and liposome-encapsulated PLP on the systemic Gr transactivation activity. Embryos (3 dpf) of the *Tg(GRE:GFP)* line were injected with free or liposome-encapsulated PLP and fluorescence microscopy images were taken at 24 hpi. A. Representative images of *Tg(GRE:GFP)* embryos injected with H₂O or 5 pmol PLP, showing the GFP signal which is a readout for the transactivation activity of Gr, which is increased after PLP injection. Scale bar = 200 μ m. B-C. The quantified GFP signals in the *Tg(GRE:GFP)* embryos at 24 hpi are shown after injection of different doses of free PLP (B), PLP encapsulated in 20% DSPG liposomes (C) and PLP encapsulated in PEGylated liposomes (D). H₂O and empty liposome were injected as control. Statistical analysis was performed by one-way ANOVA with Bonferroni's post hoc test. Significant increases in the GFP signal were observed when embryos had been injected with 0.2-5 pmol free PLP, and 1 pmol of PLP encapsulated in either 20% DSPG liposomes or in PEGylated liposomes. Each data point represents a single embryo and the means \pm s.e.m. of data accumulated from three independent experiments are shown in red. Statistically significant differences between groups are indicated by: ns, non-significant; * $p < 0.05$; **** $p < 0.0001$.

Finally, we compared all observed effects of the 1 pmol dose of free PLP and PLP encapsulated in 20% DSPG and PEGylated liposomes (Table 1). We used the ratio of the effect on neutrophil migration and the effect on regeneration or transactivation as a readout for the therapeutic ratio of the different PLP formulations. The results showed that when considering the effect on regeneration, encapsulation in 20% DSPG liposomes results in a ratio (4.707) comparable to that observed for PEGylated liposomes (4.040), which both are considerably higher than the ratio observed for free PLP (0.901). For both types of liposome, this difference with free PLP was due to both a larger inhibition of the neutrophil migration and a smaller inhibition of the regeneration. When we determined the ratio between the effect on neutrophil migration and the effect on transactivation, a higher ratio was observed for the PEGylated liposome (3.453) than for the 20% DSPG liposome (0.603), which was only slightly higher than the ratio observed for free PLP (0.177). This difference between the two types of liposomes was due to the fact that PLP in the 20% DSPG liposome had a considerably higher effect on transactivation, comparable to free PLP. In conclusion, our zebrafish model was demonstrated to be a useful model for assessing the therapeutic ratio of novel liposomal GC formulations.

Table 1. Ratio between the therapeutic effect and side effects of 1 pmol PLP treatment

Treatment	Inhibition of neutrophil migration (%) ¹		Inhibition of neutrophil migration (%)	
	Inhibition of regeneration (%)		Increase in transactivation (%)	
Free PLP	0.901	(9.8/10.9)	0.177	(9.8/55.6)
PLP in 20% DSPG liposome	4.707	(26.8/5.7)	0.603	(26.8/44.5)
PLP in PEGylated liposome	4.040	(21.4/5.3)	3.453	(21.4/6.2)

¹All effects are determined as percentage difference relative to the H₂O treatment (absolute values are shown in Figs. 4-6)

Discussion

In the present study, we have used the zebrafish embryo model to study liposomal drug targeting *in vivo*. This model enabled us to investigate the biodistribution of liposomes and to determine the anti-inflammatory effect and possible adverse effects of the glucocorticoid drug PLP encapsulated in liposomes. Our results showed that PEGylated liposomes mainly remained in the vasculature and that liposomes with a novel formulation (20% DSPG, 50% DOPC, 30% cholesterol) were mainly targeted to macrophages. Upon laser wounding, both liposomes accumulated near the wounded site, but the PEGylated liposomes showed a diffuse accumulation and the macrophage-targeting liposomes were localized inside macrophages that had been recruited to the wound. Interestingly, encapsulation of PLP in either liposome resulted in enhancement of the inhibition of neutrophil migration upon laser wounding, whereas the inhibition of tail fin regeneration and the activation of GC-responsive genes throughout the embryonic body was reduced. Thus, using our zebrafish model system we demonstrated that encapsulation of PLP in two different types of liposomes increased the anti-inflammatory effects and reduced the side effects of this GC drug.

Our results from confocal microscopy imaging of zebrafish embryos injected with different liposome formulations illustrate the feasibility to visualize and compare the biodistribution of liposomes *in vivo*, adding to previous studies on nanoparticles as a drug delivery system in zebrafish [46, 47, 52, 53]. We have investigated the biodistribution in 3 dpf embryos of the PEG2000-DSPE, DPPC and cholesterol formulation, which is widely studied for delivery of PLP [17, 18, 22, 54]. Our images show that these liposomes are mainly circulating in the vasculature at 2 hours after intravenous injection, and are hardly taken up by macrophages, in agreement with previous reports [46, 52]. For these liposomes, we observed association with endothelial cells (ECs) of the posterior cardinal vein (PCV), the caudal vein (CV) and the CHT. These venous ECs have been shown to function in zebrafish embryos as the equivalent of the liver sinusoidal/scavenger endothelial cells (LSECs) in mammals [47]. The uptake of mainly anionic nanoparticles by these cells was demonstrated to be dependent on the scavenger receptor Stabilin-2 [47]. Clearance of liposomes from the circulation by SECs, especially in the liver, is a critical problem for the application of the liposome drug delivery systems [7, 55], so we suggest to use our zebrafish model system to screen altered formulations of the PEGylated liposome for reduced association with SECs in future studies. In addition to using PEGylated liposomes, we optimized the formulation of macrophage-targeting liposomes by varying the DSPG:cholesterol ratio of a liposome that for the other 50% consisted of DOPC, with the aim to have PLP delivered to sites of inflammation by macrophages recruited to these areas. Our images show that low ratios prevent macrophage uptake and that high ratios induce more targeting to the area that includes CV and CHT, consistent with the finding that these cells preferentially scavenge anionic nanoparticles [47]. The ratio we selected for

further studies showed maximal macrophage targeting without substantial association with venous ECs.

In order to test these liposomes for the delivery of PLP to inflamed tissues, we used laser wounding in the tail of the zebrafish embryo. In previous studies we used tail fin amputation to study anti-inflammatory effects of GCs in zebrafish [51, 56], but for the present study wounding in a better vascularized part of the body seemed a more relevant model system. Both liposomes tested accumulated in the wounded area. The PEGylated liposomes, of which the accumulation is considered to depend on the EPR effect [7, 57], showed a diffuse distribution at the wounded site, whereas the macrophage-targeting liposomes were localized inside the macrophages that had migrated towards the wound. Interestingly, PLP encapsulated in either liposome type was more potent in inhibiting the wounding-induced neutrophil migration compared to free PLP. Thus, using our zebrafish model, we demonstrated an enhanced anti-inflammatory effect of PLP upon encapsulation with a new macrophage-targeting liposome formulation, and upon encapsulation in PEGylated liposomes, similarly to the enhancement observed for this type of liposomes in mammalian models [13, 16-19, 54]. The PEGylated liposome-encapsulated PLP was slightly less potent in suppressing the neutrophil migration than the PLP encapsulated in macrophage-targeting liposomes, which suggests a higher delivery efficiency of liposomes to the inflamed site through macrophage accumulation than through the EPR effect.

In order to improve GC therapies, an important aspect that should be taken into consideration is the severity of the side effects [3]. Therefore, in our study we used two *in vivo* assays to assess possible adverse effects of PLP. First, we determined the inhibition of tissue regeneration upon tail fin amputation. Inhibited wound healing or tissue regeneration is a commonly observed side effect of GC treatment [58], and the regeneration assay had also been used as a readout for side effects of GC drugs in a previous study from our lab [59]. Second, since most side effects of GCs are considered to result from the transactivation of GRE-containing promoters by activated GRs [60], we used a zebrafish reporter line in which the expression of the GFP gene was driven by a GRE-containing promoter and we determined the GFP expression throughout the body of the embryos upon administration of free PLP and encapsulated PLP [61]. The findings from both assays showed that encapsulation in either type of liposome reduced the effects of PLP, suggesting that liposome encapsulation may increase the therapeutic ratio of PLP not only by enhancing the desired anti-inflammatory effects, but also by decreasing the adverse effects. Interestingly, whereas in the tail fin regeneration assay both liposomes showed similar effects, in the GRE:GFP reporter line the macrophage-targeting liposomes showed only a slightly lower induction of the GFP expression than the PEGylated liposomes. This difference may be related to the different pharmacokinetics of the liposomes, since the effect of GCs in the tail fin

regeneration assay depends on their presence during the first hours after amputation [50, 59], whereas the observed effect on GFP expression results from their activity over almost the entire time between the injection and the imaging (24 h).

In conclusion, we present new evidence that zebrafish embryos as an animal model for studies on liposomal encapsulation of GCs are a useful tool in the development of anti-inflammatory GC therapies. Exploiting the transparency of this model, we optimized the formulation of a novel macrophage-targeting liposome and compared its biodistribution with that of a PEGylated liposome, and both liposomes showed accumulation at sites of inflammation. Encapsulation in liposomes enhanced the anti-inflammatory effects of GCs and reduce their adverse effects. These results indicate that liposome encapsulation of GCs is a promising way to increase the therapeutic ratio of these drugs, and that the zebrafish is a valuable model for future preclinical studies aimed at the optimization of liposomal formulations of anti-inflammatory GC drugs.

Materials and methods

Zebrafish lines and maintenance

Zebrafish were maintained and handled according to the guidelines from the Zebrafish Model Organism Database (<http://zfin.org>) and in compliance with the directives of the local animal welfare committee of Leiden University. They were exposed to a 14 hours light and 10 hours dark cycle to maintain circadian rhythmicity. Fertilization was performed by natural spawning at the beginning of the light period. Eggs were collected and raised at 28°C in egg water (60 µg/ml Instant Ocean sea salts and 0.0025% methylene blue). The following fish lines were used in this study: the type (wt) strain AB/TL, the transgenic lines *Tg(mpeg1:eGFP^{gl22})* [62], *Tg(mpx:GFPⁱ¹¹⁴)* [63] and *Tg(9xGCRE-HSV.U123:EGFP^{ia20})* [61].

Liposome preparation

The macrophage targeting liposomes and PEGylated liposomes were formulated in ddH₂O and Phosphate-buffered saline (PBS) respectively at a total lipid concentration of 5 mM [32, 47]. Stock solutions of lipids (in chloroform) were mixed at specific molar ratios, dried and rehydrated in 1 mL ddH₂O. Liposomes with a size of 100 nm were formed through extrusion (Mini-extruder with heating block, Avanti Polar Lipids, Alabaster, US) using the polycarbonate membranes with corresponding pore size, and stored at 4 °C. The macrophage targeting liposomes consisted of DSPG, DOPC and cholesterol, with molar ratios of either 10:50:40, 15:50:35, 20:50:30, 25:50:35 or 30:50:20. The PEGylated liposomes consisted of dipalmitoyl phosphatidyl choline (DPPC), PEG 2000 distearoyl

phosphatidylethanolamine (PEG-DSPE) and cholesterol with a molar ratio of 62:5:33. Prednisolone phosphate (PLP, MedChemExpress) was encapsulated by hydrating the lipid film with an aqueous solution of 50mg/ml PLP. After extrusion the unencapsulated PLP was removed by size exclusion chromatography and the encapsulated amount was determined by the absorbance measured by UV spectrophotometry. Reported amounts of PLP are total amounts in the solution. All liposomes (with or without encapsulated PLP) were prepared freshly before injection.

Injection of drugs

All treatments were given intravenously to the zebrafish embryos. After anesthesia with 0.02% aminobenzoic acid ethyl ester (tricaine, Sigma-Aldrich), 2 or 3 dpf embryos were injected with control solution (water), empty liposomes, different amounts of free PLP or liposome encapsulated PLP in the duct of Cuvier under a Leica M165C stereomicroscope. For free PLP, the injected volume was 1 nl and the concentration of the injected PLP solution (in ddH₂O) varied from 25 mM PLP to 0.04 mM to achieve an injected amount of 25 pmol to 0.04 pmol. For liposome-encapsulated PLP, the injected amount of 1 pmol was achieved by injecting the original liposome solution with a volume calculated based on the concentration determined by UV spectrophotometry. Lower doses were injected using the same volume and a lower concentration of liposomes. As a control for testing the vascular permeability, 1nl of 20 µg/ml dextran was injected (fluorescently labeled with tetramethylrhodamine, 2,000,000 MW, Invitrogen).

Microscopy

For confocal laser scanning microscopy, anesthetized embryos were mounted in 1% low melting agarose in egg water containing 0.02% tricaine on 40 mm glass-bottom dishes (WillCo-dish, WillCo Wells). Images were taken using a Leica TCS SP8 confocal microscope with a 10X (NA 0.4), or 20X (NA 0.75) objective (Figure 1-3, Supplementary Figure 2). For other brightfield and/or fluorescence microscopy imaging, anesthetized embryos were imaged using a Leica M205FA fluorescence stereomicroscope, equipped with a Leica DFC 345FX camera (Figure 4-6).

Laser wounding

Adapted from the method of yolk wounding using laser irradiation in zebrafish embryos described previously [64], we used laser wounding to a region in the tail, since this area is vascularized and the thin tissue allows convenient imaging of accumulated leukocytes. Anesthetized 3 dpf embryos were mounted in 1% low melting agarose in egg water containing 0.02% tricaine on a microscope slide (VWR). A 100 µm long burning wound was created in the tail by laser irradiation with a ZEISS PALM

Microbeam Laser Microdissection system using a 20X objective (NA 0.4) (Figure 3A). Drug treatment by intravenous injection was performed immediately after wounding. The number of recruited neutrophils was determined at 4 hours after wounding.

Regeneration assay

The tails of anesthetized 2dpf embryos were partially amputated with a 1 mm sapphire blade (World Precision Instruments) on 2% agarose-coated Petri dishes under a Leica M165C stereomicroscope (Figure 5A). Drug treatment by intravenous injection was performed immediately after amputation. The length of fin regeneration was determined from microscopic images taken at 36 hpa as previously described [50].

Image analysis

To determine neutrophil migration upon laser wounding, neutrophils were detected based on their fluorescent GFP label, and to quantify the number of recruited neutrophils in the fluorescence microscopy images of the wounded tails, the cells in a defined area of the tail were counted manually (Figure 4A). For the quantitation of the regeneration assay, in the images of the tail fins the length of the regenerated tissue was determined from the center of the original plane of amputation to the tip of the regenerating fin (Figure 5). Quantitation of transactivation of a GRE-containing promoter in the *Tg(9xGRE-HSV.U123:EGFP^{ia20})* was done on images taken at 24hpi, by determining the relative EGFP signal in the embryonic body using the Analyze and Measure tool in the ImageJ software, and determining the value "RawIntDen" (the sum of the values of the pixels in the image) (Figure 6A).

Statistical analysis

Statistical analysis was performed using GraphPad Prism 7 by one-way ANOVA with Bonferroni's post hoc test (Figures 1,2,4-6) or two-tailed t-test (Figure 3F). Significance was accepted at $p < 0.05$.

Acknowledgements

We thank Lukas Wijaya, Olga Snip, Chantal Pont and Dr. Johan Kuiper for their assistance with the Microbeam Laser Microdissection system. We thank the fish facility team, in particular Guus van der Velden, Natasha Montiadi, Ulrike Nehrdich and Ruth van Koppen for zebrafish maintenance. We thank Dr. Graham Lieschke, Dr. Stephen A. Renshaw and Dr. Luisa Dalla Valle for providing transgenic zebrafish lines.

References

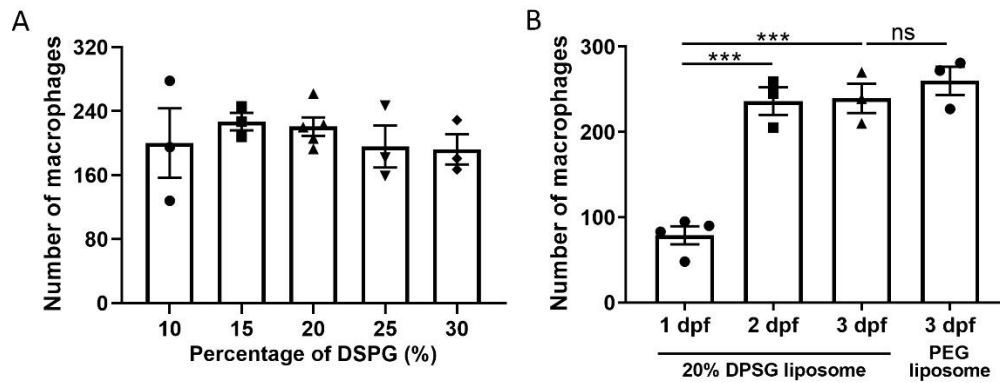
1. Busillo, J.M. and J.A. Cidlowski, *The five Rs of glucocorticoid action during inflammation: ready, reinforce, repress, resolve, and restore*. Trends in Endocrinology & Metabolism, 2013. **24**(3): p. 109-119.
2. Barnes, P.J., *Glucocorticosteroids: current and future directions*. British Journal of Pharmacology, 2011. **163**(1): p. 29-43.
3. Moghadam-Kia, S. and V.P. Werth, *Prevention and treatment of systemic glucocorticoid side effects*. International journal of dermatology, 2010. **49**(3): p. 239-248.
4. Yasir, M. and S. Sonthalia, *Corticosteroid adverse effects*. 2019.
5. Ulbrich, W. and A. Lamprecht, *Targeted drug-delivery approaches by nanoparticulate carriers in the therapy of inflammatory diseases*. Journal of The Royal Society Interface, 2010. **7**(suppl_1): p. S55-S66.
6. Bardania, H., S. Tarvirdipour, and F. Dorkoosh, *Liposome-targeted delivery for highly potent drugs*. Artificial Cells, Nanomedicine, and Biotechnology, 2017. **45**(8): p. 1478-1489.
7. Nehoff, H., et al., *Nanomedicine for drug targeting: strategies beyond the enhanced permeability and retention effect*. International journal of nanomedicine, 2014. **9**: p. 2539.
8. Decuzzi, P., et al., *Size and shape effects in the biodistribution of intravascularly injected particles*. Journal of Controlled Release, 2010. **141**(3): p. 320-327.
9. Taurin, S., H. Nehoff, and K. Greish, *Anticancer nanomedicine and tumor vascular permeability; where is the missing link?* Journal of controlled release, 2012. **164**(3): p. 265-275.
10. Bae, Y.H. and K. Park, *Targeted drug delivery to tumors: myths, reality and possibility*. Journal of controlled release, 2011. **153**(3): p. 198.
11. Voinea, M. and M. Simionescu, *Designing of 'intelligent' liposomes for efficient delivery of drugs*. Journal of cellular and molecular medicine, 2002. **6**(4): p. 465-474.
12. Tiwari, G., et al., *Drug delivery systems: An updated review*. International journal of pharmaceutical investigation, 2012. **2**(1): p. 2.
13. Schmidt, J., et al., *Drug targeting by long - circulating liposomal glucocorticosteroids increases therapeutic efficacy in a model of multiple sclerosis*. Brain, 2003. **126**(8): p. 1895-1904.
14. Grigoletto, A., et al., *Drug and protein delivery by polymer conjugation*. Journal of Drug Delivery Science and Technology, 2016. **32**: p. 132-141.
15. Yan, X., G.L. Scherphof, and J.A. Kamps, *Liposome opsonization*. Journal of liposome research, 2005. **15**(1-2): p. 109-139.
16. Metselaar, J.M., et al., *Complete remission of experimental arthritis by joint targeting of glucocorticoids with long - circulating liposomes*. Arthritis & Rheumatism: Official Journal of the American College of Rheumatology, 2003. **48**(7): p. 2059-2066.
17. Hofkens, W., et al., *Intravenously delivered glucocorticoid liposomes inhibit osteoclast activity and bone erosion in murine antigen-induced arthritis*. Journal of controlled release, 2011. **152**(3): p. 363-369.
18. Metselaar, J.v., et al., *Liposomal targeting of glucocorticoids to synovial lining cells strongly increases therapeutic benefit in collagen type II arthritis*. Annals of the rheumatic diseases, 2004. **63**(4): p. 348-353.
19. Lobatto, M.E., et al., *Multimodal clinical imaging to longitudinally assess a nanomedical anti-inflammatory treatment in experimental atherosclerosis*. Molecular pharmaceutics, 2010. **7**(6): p. 2020-2029.
20. Schiffelers, R.M., et al., *Liposome-encapsulated prednisolone phosphate inhibits growth of established tumors in mice*. Neoplasia, 2005. **7**(2): p. 118-127.
21. Banciu, M., et al., *Liposomal glucocorticoids as tumor-targeted anti-angiogenic nanomedicine in B16 melanoma-bearing mice*. The Journal of steroid biochemistry and molecular biology, 2008. **111**(1-2): p. 101-110.

22. Hofkens, W., et al., *Safety of glucocorticoids can be improved by lower yet still effective dosages of liposomal steroid formulations in murine antigen-induced arthritis: comparison of prednisolone with budesonide*. International journal of pharmaceutics, 2011. **416**(2): p. 493-498.
23. van den Hoven, J.M., et al., *Optimizing the therapeutic index of liposomal glucocorticoids in experimental arthritis*. International journal of pharmaceutics, 2011. **416**(2): p. 471-477.
24. Meka, R.R., et al., *Peptide-targeted liposomal delivery of dexamethasone for arthritis therapy*. Nanomedicine, 2019. **14**(11): p. 1455-1469.
25. Verma, A., et al., *Folate conjugated double liposomes bearing prednisolone and methotrexate for targeting rheumatoid arthritis*. Pharmaceutical Research, 2019. **36**(8): p. 123.
26. Poh, S., et al., *Selective liposome targeting of folate receptor positive immune cells in inflammatory diseases*. Nanomedicine: Nanotechnology, Biology and Medicine, 2018. **14**(3): p. 1033-1043.
27. Gaillard, P.J., et al., *Enhanced brain delivery of liposomal methylprednisolone improved therapeutic efficacy in a model of neuroinflammation*. Journal of controlled release, 2012. **164**(3): p. 364-369.
28. Sylvester, B., et al., *Optimization of prednisolone-loaded long-circulating liposomes via application of Quality by Design (QbD) approach*. Journal of liposome research, 2018. **28**(1): p. 49-61.
29. Lobatto, M.E., et al., *Pharmaceutical development and preclinical evaluation of a GMP-grade anti-inflammatory nanotherapy*. Nanomedicine: nanotechnology, biology and medicine, 2015. **11**(5): p. 1133-1140.
30. Patras, L., et al., *Liposomal prednisolone phosphate potentiates the antitumor activity of liposomal 5-fluorouracil in C26 murine colon carcinoma in vivo*. Cancer biology & therapy, 2017. **18**(8): p. 616-626.
31. Smits, E.A.W., et al., *The availability of drug by liposomal drug delivery : Individual kinetics and tissue distribution of encapsulated and released drug in mice after administration of PEGylated liposomal prednisolone phosphate*. Investigational new drugs, 2019. **37**(5): p. 890-901.
32. van der Valk, F.M., et al., *Prednisolone-containing liposomes accumulate in human atherosclerotic macrophages upon intravenous administration*. Nanomedicine: nanotechnology, biology and medicine, 2015. **11**(5): p. 1039-1046.
33. Turk, M.J., D.J. Waters, and P.S. Low, *Folate-conjugated liposomes preferentially target macrophages associated with ovarian carcinoma*. Cancer letters, 2004. **213**(2): p. 165-172.
34. Tie, Y., et al., *Targeting folate receptor β positive tumor-associated macrophages in lung cancer with a folate-modified liposomal complex*. Signal transduction and targeted therapy, 2020. **5**(1): p. 1-15.
35. Chono, S., et al., *Uptake characteristics of liposomes by rat alveolar macrophages: influence of particle size and surface mannose modification*. Journal of pharmacy and pharmacology, 2007. **59**(1): p. 75-80.
36. Düffels, A., et al., *Synthesis of high -mannose type neoglycolipids: Active targeting of liposomes to macrophages in gene therapy*. Chemistry—A European Journal, 2000. **6**(8): p. 1416-1430.
37. Andersen, M.N., et al., *STAT3 inhibition specifically in human monocytes and macrophages by CD163-targeted corosolic acid-containing liposomes*. Cancer Immunology, Immunotherapy, 2019. **68**(3): p. 489-502.
38. Tentillier, N., et al., *Anti-inflammatory modulation of microglia via CD163-targeted glucocorticoids protects dopaminergic neurons in the 6-OHDA Parkinson's disease model*. Journal of Neuroscience, 2016. **36**(36): p. 9375-9390.
39. Montes-Cobos, E., et al., *Targeted delivery of glucocorticoids to macrophages in a mouse model of multiple sclerosis using inorganic-organic hybrid nanoparticles*. Journal of Controlled Release, 2017. **245**: p. 157-169.

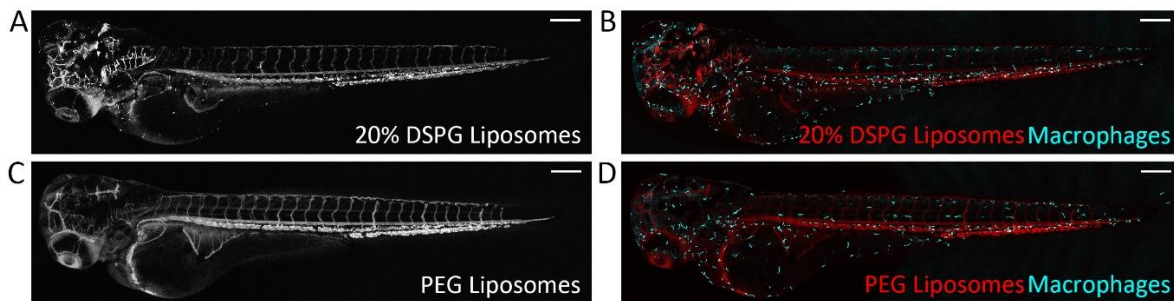
40. Howe, K., et al., *The zebrafish reference genome sequence and its relationship to the human genome*. Nature, 2013. **496**(7446): p. 498-503.
41. Doudna, J.A. and E. Charpentier, *The new frontier of genome engineering with CRISPR-Cas9*. Science, 2014. **346**(6213).
42. Lewis, K.L., N. Del Cid, and D. Traver, *Perspectives on antigen presenting cells in zebrafish*. Developmental & Comparative Immunology, 2014. **46**(1): p. 63-73.
43. Schaaf, M., A. Chatzopoulou, and H. Spaink, *The zebrafish as a model system for glucocorticoid receptor research*. Comparative Biochemistry and Physiology Part A: Molecular & Integrative Physiology, 2009. **153**(1): p. 75-82.
44. Alsop, D. and M.M. Vijayan, *Development of the corticosteroid stress axis and receptor expression in zebrafish*. Am J Physiol Regul Integr Comp Physiol, 2008. **294**(3): p. R711-9.
45. Schaaf, M.J., et al., *Discovery of a functional glucocorticoid receptor beta-isoform in zebrafish*. Endocrinology, 2008. **149**(4): p. 1591-9.
46. Sieber, S., et al., *Zebrafish as a predictive screening model to assess macrophage clearance of liposomes in vivo*. Nanomedicine: Nanotechnology, Biology and Medicine, 2019. **17**: p. 82-93.
47. Campbell, F., et al., *Directing nanoparticle biodistribution through evasion and exploitation of Stab2-dependent nanoparticle uptake*. ACS nano, 2018. **12**(3): p. 2138-2150.
48. Ringdén, O., et al., *Efficacy of amphotericin B encapsulated in liposomes (AmBisome) in the treatment of invasive fungal infections in immunocompromised patients*. J Antimicrob Chemother, 1991. **28 Suppl B**: p. 73-82.
49. Cornely, O.A., et al., *Liposomal amphotericin b as initial therapy for invasive mold infection: a randomized trial comparing a high-loading dose regimen with standard dosing (AmBiLoad Trial)*. Clinical infectious diseases, 2007. **44**(10): p. 1289-1297.
50. Mathew, L.K., et al., *Unraveling tissue regeneration pathways using chemical genetics*. Journal of Biological Chemistry, 2007. **282**(48): p. 35202-35210.
51. Chatzopoulou, A., et al., *Glucocorticoid-induced attenuation of the inflammatory response in zebrafish*. Endocrinology, 2016. **157**(7): p. 2772-2784.
52. Sieber, S., et al., *Zebrafish as an early stage screening tool to study the systemic circulation of nanoparticulate drug delivery systems in vivo*. Journal of Controlled Release, 2017. **264**: p. 180-191.
53. Fenaroli, F., et al., *Nanoparticles as drug delivery system against tuberculosis in zebrafish embryos: direct visualization and treatment*. ACS nano, 2014. **8**(7): p. 7014-7026.
54. Hofkens, W., et al., *Liposomal targeting of prednisolone phosphate to synovial lining macrophages during experimental arthritis inhibits M1 activation but does not favor M2 differentiation*. PloS one, 2013. **8**(2): p. e54016.
55. Immordino, M.L., F. Dosio, and L. Cattel, *Stealth liposomes: review of the basic science, rationale, and clinical applications, existing and potential*. International journal of nanomedicine, 2006. **1**(3): p. 297.
56. Xie, Y., et al., *Glucocorticoids inhibit macrophage differentiation towards a pro-inflammatory phenotype upon wounding without affecting their migration*. Disease models & mechanisms, 2019. **12**(5).
57. Maeda, H., et al., *Tumor vascular permeability and the EPR effect in macromolecular therapeutics: a review*. Journal of controlled release, 2000. **65**(1-2): p. 271-284.
58. Slominski, A.T. and M.A. Zmijewski, *Glucocorticoids inhibit wound healing: novel mechanism of action*. Journal of Investigative Dermatology, 2017. **137**(5): p. 1012-1014.
59. He, M., et al., *Ginsenoside Rg1 Acts as a Selective Glucocorticoid Receptor Agonist with Anti-Inflammatory Action without Affecting Tissue Regeneration in Zebrafish Larvae*. Cells, 2020. **9**(5): p. 1107.
60. Schäcke, H., W.-D. Döcke, and K. Asadullah, *Mechanisms involved in the side effects of glucocorticoids*. Pharmacology & therapeutics, 2002. **96**(1): p. 23-43.

61. Benato, F., et al., *A living biosensor model to dynamically trace glucocorticoid transcriptional activity during development and adult life in zebrafish*. *Molecular and cellular endocrinology*, 2014. **392**(1-2): p. 60-72.
62. Ellett, F., et al., *mpeg1 promoter transgenes direct macrophage-lineage expression in zebrafish*. *Blood*, 2011. **117**(4): p. e49-e56.
63. Renshaw, S.A., et al., *A transgenic zebrafish model of neutrophilic inflammation*. *Blood*, 2006. **108**(13): p. 3976-3978.
64. Redd, M.J., et al., *Imaging macrophage chemotaxis in vivo: studies of microtubule function in zebrafish wound inflammation*. *Cell motility and the cytoskeleton*, 2006. **63**(7): p. 415-422.

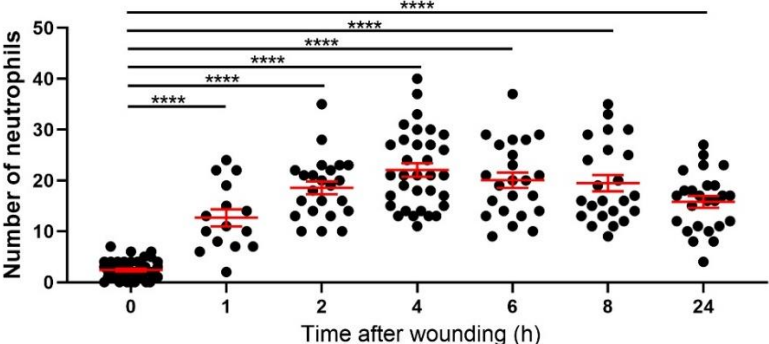
Supplementary material



Supplementary Figure 1. The number of macrophages in the whole body of embryos. *Tg(mpeg1:GFP)* embryos were injected with liposomes containing different percentages of DSPG at 2 days post fertilization (dpf) (A) or 20% DSPG liposomes at 1, 2 and 3 dpf and PEGylated liposomes at 3dpf (B). Confocal microscopy images were taken at 2 hours post injection (hpi) and the number of macrophages over the whole body was quantified. Statistical analysis was performed by one-way ANOVA with Bonferroni's post hoc test. No significant differences were observed in panel A. In panel B, no significant difference was observed when injected with 20% DSPG liposome and PEG liposome at 3 dpf. Upon injection with 20% DSPG liposomes, at 2 dpf and 3 dpf significantly higher numbers of macrophages were observed than at 1 dpf. Data shown are the means \pm s.e.m. of 3-5 individual embryos, of which the individual data are indicated. Statistically significant differences between groups are indicated by: ns, non-significant; *** $p < 0.001$.



Supplementary Figure 2. Biodistribution in zebrafish embryos of liposomes encapsulating PLP. A-B. Representative confocal microscopy images of 3 dpf embryos of the *Tg(mpeg1:GFP)* line injected with 20% DSPG (A) or PEGylated (B) liposomes encapsulating PLP. Images were taken at 2 hpi. Liposomes are shown in red and macrophages in cyan. Scale bar = 200 μ m.



Supplementary Figure 3. Number of neutrophils recruited to the wounded area at different time points after laser wounding. Embryos (at 3 dpf) of the *Tg(mpx:GFP)* line were subjected to laser wounding, and fluorescence microscopy images were taken at different time points after the wounding procedure. The number of neutrophils recruited to the wounded area are shown. Statistical analysis was performed by one-way ANOVA with Bonferroni's post hoc test. Each data point represents a single embryo and the means \pm s.e.m. of data accumulated from three independent experiments are shown in red. Statistically significant differences between groups are indicated by: **** $p < 0.0001$.

